TPX2 Promotes Metastasis and Serves as a Marker of Poor Prognosis in Non-Small Cell Lung Cancer

Authors' Contribution:
Study Design A
Data Collection B
Statistical Analysis C
Data Interpretation D
Manuscript Preparation E
Literature Search F
Funds Collection G

ACE 1 **Fang Zhou**
D 1 **Meng Wang**
F 2 **Mijiti Aibaidula**
D 2 **Zhiguo Zhang**
B 2 **Abudusaimaiti Aihemaiti**
B 2 **Rezhake Aili**
B 2 **Hao Chen**
B 2 **Shuangfeng Dong**
B 2 **Wei Wei**
ACG 2 **Abulizi Maimaitiaili**

1 Department of Thoracic Surgery, Tianjin Chest Hospital, Tianjin, P.R. China
2 Department of Cardiothoracic Surgery, People's Hospital of Hetian, Hetian, Xinjiang, P.R. China

Corresponding Author:
Abulizi Maimaitiaili, e-mail: abliz2010@hotmail.com

Background:
Metastasis contributes to the high mortality rate of non-small cell lung cancer (NSCLC), and gaining a better understanding of its metastatic mechanisms would aid in initiating effective clinical treatment.

Material/Method:
In this study, bioinformatics analyses of the GEO database and TCGA-LUAD were first used to identify the key node gene regulating NSCLC malignant progression. Further *in vitro* experiments, including wound healing assay, invasion assay, Western blot assay, and luciferase report assay, were used to clarify the functions and mechanism of TPX2 in NSCLC.

Results:
Results of the TCGA analysis showed that TPX2 was significantly positively correlated with tumor metastasis and growth and the clinical stage of NSCLC. In addition, high levels of TPX2 significantly indicated a poor survival rate. *In vitro* experimental results also revealed that the upregulation of TPX2 significantly promoted NSCLC cell migration and invasion and could affect cell replasticity. Further results indicated that TPX2 significantly activated the epithelial-mesenchymal transition process and promoted the expression and activities of matrix metalloproteinase (MMP)2 and MMP9.

Conclusions:
This study demonstrated that TPX2 promotes the metastasis and malignant progression of NSCLC and could thus serve as a marker of poor prognosis in NSCLC.

MeSH Keywords:
Carcinoma • Carcinoma, Non-Small-Cell Lung • Neoplasm Metastasis

Full-text PDF:
https://www.medscimonit.com/abstract/index/idArt/925147

📄 2440   ▦ 1   📊 6   📚 25

Background

Lung cancer ranks as the leading cause of cancer-related deaths worldwide. Non-small cell lung cancer (NSCLC) is one type of lung cancer, and it has a high incidence rate, accounting for about 85% of all lung cancers [1,2]. Patients with NSCLC usually have a poor prognosis due to diagnosis at an advanced stage [3]. More than 1.5 million deaths are caused by metastatic NSCLC each year, and these place a heavy burden on social health [1]. Only a small number of early-stage NSCLC patients can be treated with surgery and achieve a high 5-year survival rate. For more advanced NSCLC, chemotherapy and radiotherapy are suggested, but the 5-year survival rate is only ~23%. Immunological, radiotherapy, and targeted therapies are associated with some success in treating advanced NSCLC, but there are still limitations precluding their uses in some cases [4–8]. For immunological therapies, targeting activity is the key to successful treatment, but a high treatment cost restricts the further promotion of this therapy [9]. Thus, a better understanding of the mechanisms of NSCLC metastasis is urgently needed to advance clinical treatments for patients with the disease.

Circulating tumor cells (CTCs) represent a pattern of blood-borne metastasis, which is a necessary way for tumors to become established at distant sites [10]. Gene expression profile data can reflect the changes of functions and signaling pathways in cells and thus reveal the pathological mechanisms underlying various diseases [11–13]. In the present study, the GEO database of GSE50991 containing mRNA expression profiles of circulating and non-metastatic lung tumor cells was used [14]. By investigating differential gene expression and function and conducting signaling pathway enrichment analyses [15], we identified *TPX2* as the key regulatory gene in NSCLC metastasis and malignant progression. *TPX2* overexpression has been found in a wide range of tumor types, including bladder, cervical, gastric, and hepatocellular carcinoma cancers [16–19]. Although several studies have shown that *TPX2* contributes to cell proliferation and apoptosis of lung cancer [20], whether it plays an important role in the metastasis and malignant progression of NSCLC and what the underlying mechanism might be remain unclear.

In this study, we aimed to identify the key node gene in regulating the metastasis and malignant progression of NSCLC and then to verify the relationship between TPX2 and the clinicopathological features of NSCLC. We also aimed to further clarify the molecular mechanisms of TPX2 on cell metastasis in NSCLC.

Material and Methods

Analysis of mRNA expression profiles

The mRNA expression profile of GSE50991 was downloaded from the GEO database for use in this study [14]. Nine independent experiments were conducted to compare the mRNA expression profiles of circulating and nonmetastatic NSCLC tumor cells separately. We set the cutoff limit of |log2fold change| ≥2 for the differentially expressed genes (DEGs). The R packages pheatmap and limma were used to analyze the DEGs among these 18 groups. The DEGs were further subjected to function and pathway analyses. The protein-protein interaction (PPI) annotation and visualization were retrieved using the STRING database and Cytoscape software. The Cytoscape apps CentiScape and MCODE were used for further topological analysis. The GO and KEGG pathway analyses were conducted by using the Metascape website (*https://metascape.org*), while the enriched functions and pathways were visualized through the R package of ggplot2. The gene set enrichment analysis (GSEA) of total mRNA expression profiles was conducted using the R packages of clusterProfiler, enrichplot, and ggplot2 [21].

Analysis of the TCGA data

The RNA-seq gene expression data of 594 samples (535 LUAD samples and 59 normal tissue samples) generated by Illumina HiSeq were obtained from The Cancer Genome Atlas (TCGA). The clinical information associated with samples was downloaded from the GDC data portal. The immunochemistry results of TPX2 in NSCLC were obtained from the open website of The Human Protein Atlas (*https://www.proteinatlas.org/*). The clinical analysis of TPX2 in NSCLC was conducted by combining the TCGA and Protein Atlas-downloaded data (Supplementary Table 1). We set the median value as the dividing point for high expression and low expression of TPX2 in the clinical analyses.

Cell culture and transfection

The NSCLC cells of A549, H1975, H1299, H522, and H1650 were cultured in RPMI-1640 medium supplemented with 10% fetal bovine serum (Hyclone) and penicillin (50 µg/mL) plus streptomycin (50 µg/mL). All cultures were maintained under a humidified atmosphere containing 5% CO_2. When cells reached an acceptable density, the TPX2 overexpression plasmid and shTPX2 knockdown plasmid were transfected into NSCLC cells with the transfection reagent (Roche, Switzerland), separately. The images of cells were visualized using a microscope (Nikon, Japan).

Wound healing assays

Treated NSCLC cells were seeded into 24-well culture plates at a density of 5×10^5 cells/well. After about 12 h of incubation, a 200 µL pipette tip was used to scratch a wound into the surface. After incubation with serum-free medium for another 48 h, images of the healing were taken. All experiments were performed at least in triplicate, and mean±SD values are presented.

Invasion assays

Treated NSCLC cells were diluted with serum-free medium at a concentration of 1×10^5 cells/mL, and 200 µL of the diluted medium was then added to a Matrigel-coated top chamber. After 48 h of invasion in a humidified atmosphere containing 5% CO_2, the passed cells were fixed in 4% paraformaldehyde and stained with crystal violet solution, and images of the passed NSCLC cells were then taken. All experiments were performed at least in triplicate, and the mean ± SD values are presented.

Western blotting

The total proteins in treated cells were isolated by using the RIPA lysate buffer, and the protein concentrations were measured by bicinchoninic acid (BCA) protein assay kit (Thermo, USA). Western blotting was performed through sodium dodecyl sulfate polyacrylamide gel electrophoresis and subsequent transfer to polyvinylidene difluoride membranes. The membranes were then probed with primary antibodies of TPX2, E-cad, claudin 3, vimentin, fibronectin, or GAPDH, followed by incubation with a corresponding second antibody (1: 10 000, Santa Cruz Biotechnology, USA). All primary antibodies were purchased from Abcam and incubated with 1: 1000 dilutions. Densitometric analysis was performed by using the ImageJ software. All experiments were performed at least in triplicate, and the mean±SD values are presented.

Luciferase reporter assays

The luciferase reporter plasmids (GeneCopoeia, China) were designed by inserting the promoter clones for the matrix metalloproteinase 2 (*MMP2*) or *MMP9* gene to the vector of pE-ZX-PG04.1 with the tracking gene of secreted alkaline phosphatase. After cotransfection of the MMP2 or MMP9 luciferase reporter plasmid and TPX2 overexpression or knockdown plasmid, the NSCLC cells were incubated for another 48 h in a humidified atmosphere containing 5% CO_2. Fluorescence detection was performed by using the Dual-Luciferase Assays System (Promega) with a Luminescent reader system. All experiments were performed at least in triplicate, and the mean±SD values are presented.

MMP activity assays

The MMP activity assays were performed by using the MMP activity assay kit (Abcam, USA). The media collected from treated NSCLC cells were incubated with the APMA working solution for about 15 min at room temperature. Then, the MMP Green Substrate solution was added and incubated for another 1 h at 37°C. Fluorescence detection was performed by using a microplate reader system at wavelengths of 490 and 595 nm. All experiments were performed at least in triplicate, and the mean±SD values are presented.

Statistical analysis

IBM SPSS Statistics 22.0 software (Chicago, IL, USA) was used to perform statistical analyses. Gap closure was analyzed by one-way ANOVA followed by pairwise comparison with the control groups by paired *t* test. All data are presented as mean±SD. All experiments were performed at least in triplicate, and $P < 0.05$ was considered statistically significant.

Results

Selection of the key candidate gene in regulating the malignant progression of NSCLC

mRNA expression profile data downloaded from the GEO database were used to screen for the key candidate gene. The heatmap analysis results showed very different expressed gene profiles between the circulating tumor cells and non-metastatic tumor cells of NSCLC (Figure 1A). The volcano plot further described the DEGs between these 2 groups, in which many genes were significantly upregulated, whereas others were significantly downregulated (Figure 1B). To screen for the key candidate gene regulating the malignant progression of NSCLC, the upregulated genes were subjected to PPI analysis. The constructed PPI network considered 601 nodes and 2416 edges (Figure 1C, left). By using the Cytoscape APPs of CentiScape and MCODE, we further screened the topological network with features of Degree and K-core, and a hub network was identified with the MCODE-score of 21.478 (Figure 1C, right). As a result, the potential hub node of *TPX2* was identified as a candidate gene in regulating the malignant progression of NSCLC.

TPX2 promotes metastasis and malignant progression of NSCLC

To explore the correlation between TPX2 expression and NSCLC, the LUAD dataset from TCGA was analyzed. The TPX2 immunochemistry results showed a remarkable increase of TPX2 expression in metastatic lung cancer tissues compared with non-metastatic lung cancer tissues (Figure 2A). Statistical results
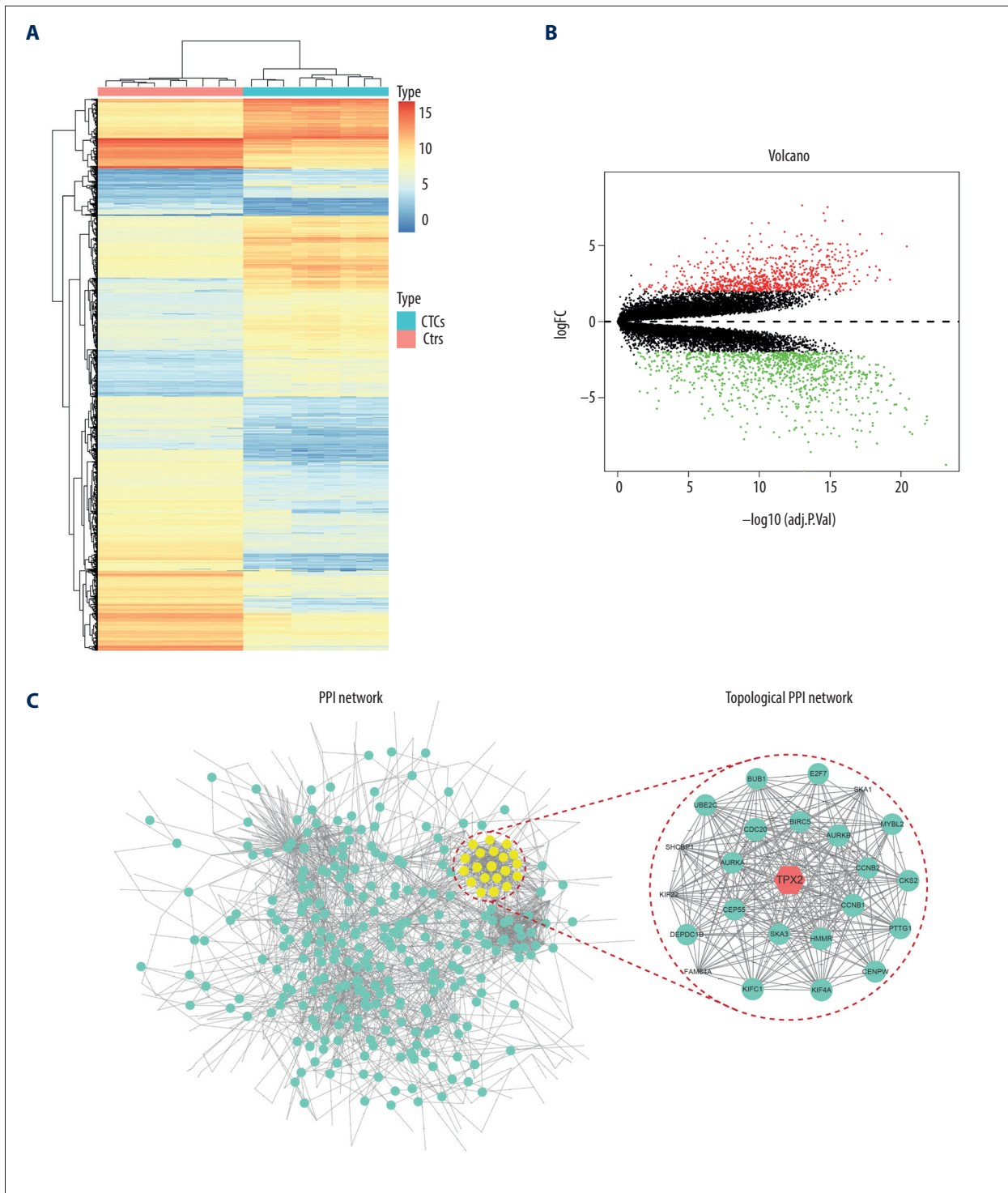
Figure 1. TPX2 was selected as the key candidate gene in regulating the malignant progression of NSCLC. (**A**) Heatmap analysis of DEGs revealed a substantial difference between circulating and nonmetastatic NSCLC tumor cells. (**B**) Volcano plot for the DEGs between circulating and nonmetastatic NSCLC tumor cells, where the red and green plots indicating the upregulated and downregulated genes, respectively. (**C**) PPI network analysis of DEGs revealed NSCLC-related PPI hubs, and topological PPI network indicated TPX2 as a key node gene. DEGs – differentially expressed genes; CTCs – circulating tumor cells; Ctrl – nonmetastatic NSCLC tumor cells; PPI – protein–protein interaction.
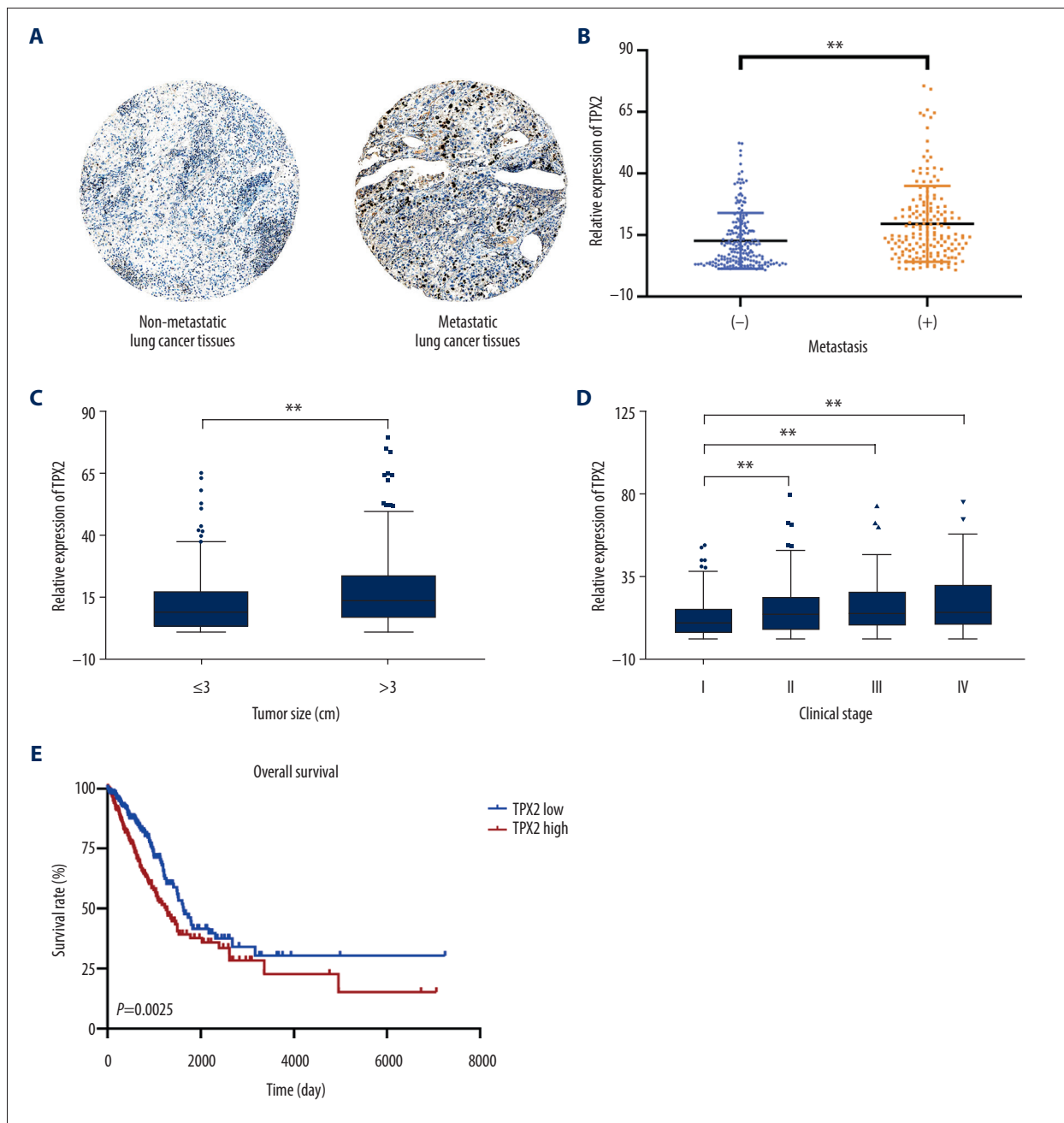
Figure 2. Correlation of TPX2 with NSCLC tumor characteristics in clinical samples. (**A**) TPX2 staining was weakly positive and strongly positive in nonmetastatic and metastatic lung cancer tissues, separately. (**B**) TPX2 expression was significantly upregulated in the metastatic NSCLC samples compared with the nonmetastatic NSCLC samples. (**C**) TPX2 expression was significantly increased with the NSCLC tumor size. (**D**) TPX2 expression was significantly increased with the NSCLC clinical stage. (**E**) Overall survival analysis of TPX2 on patients with NSCLC (mean±SD; ** $P<0.01$).
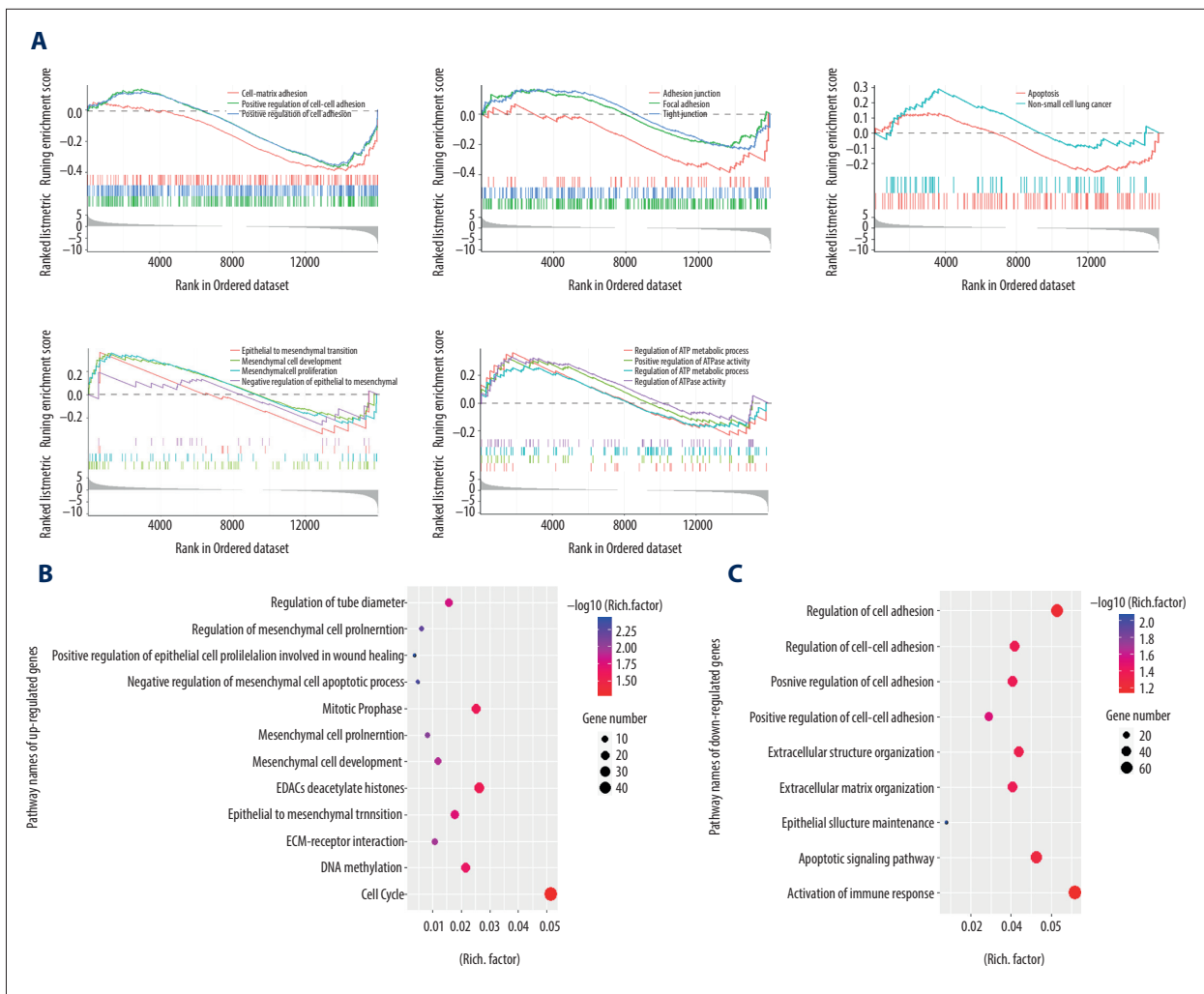
Figure 3. Function and pathway analyses of the mRNA expression profiles. (**A**) GSEA results of total mRNA showed differential regulation among cell adhesion, EMT, and ATP metabolism. (**B**) GO and KEGG analyses of the upregulated genes. (**C**) GO and KEGG analyses of the downregulated genes. GSEA – Gene Set Enrichment Analysis; GO – Gene Ontology; KEGG – Kyoto Encyclopedia of Genes and Genomes.

showed that TPX2 expression was significantly increased when lung cancer cells metastasized (Figure 2B). Similarly, TPX2 expression had significantly positive correlations with tumor size (Figure 2C) and clinical stage (Figure 2D). Further analysis revealed that NSCLC patients with high TPX2 expression had a significantly lower survival rate compared with those with low TPX2 expression (P=0.0025, Figure 2E).

TPX2 affects migration, invasion, and cell replasticity in NSCLC

To clarify the exact role of TPX2 in NSCLC, the mRNA expression profile data were subjected to GSEA analysis. The GSEA results showed that when metastasis occurred, the junction between cell and cell or that between cell and matrix decreased; the regulation of apoptosis decreased, while the malignant

progression of NSCLC increased; and the epithelial-mesenchymal transition (EMT) process and ATP generation increased (Figure 3A). The DEGs were further subjected to GO and KEGG analyses, and the results were consistent with the GSEA results. The pathways and functions associated with the upregulated genes included the regulation of tube diameter, the EMT process, and the cell cycle (Figure 3B). Meanwhile, the pathways and functions associated with downregulated genes were cell adhesion, extracellular matrix organization, and the apoptosis signaling pathway (Figure 3C).

Based on the omics analysis results, we suspected that TPX2 might play an important role in regulating NSCLC metastasis. Thus, we designed *in vitro* experiments for verification. First, 5 NSCLC cell lines were chosen to detect the background expression levels of TPX2. A549 and H1650 were separately
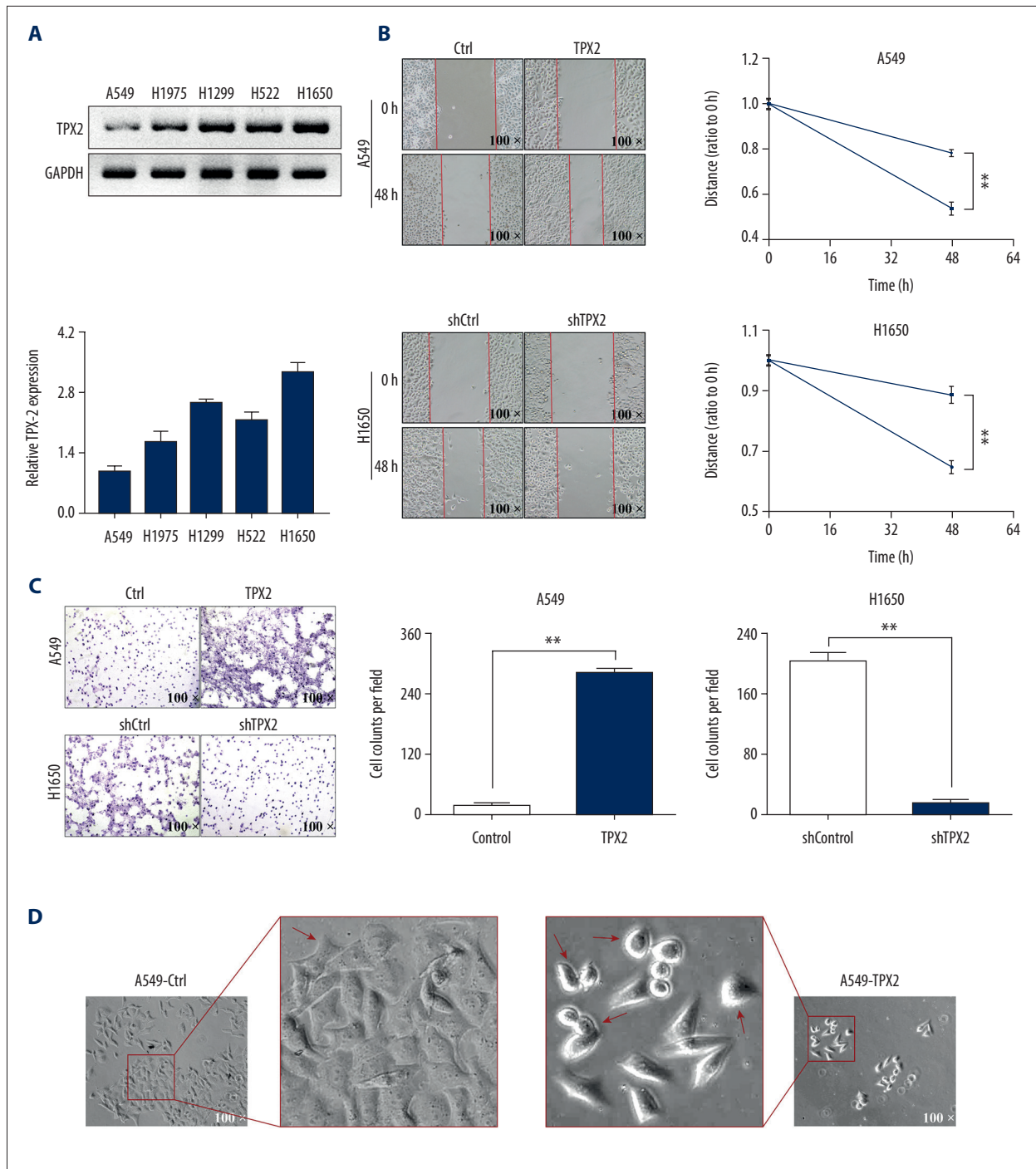
Figure 4. TPX2 affected NSCLC migration, invasion, and cell replasticity. (**A**) Relative TPX2 expression analysis in 5 NSCLC cell lines; the ratio of densitometry value to the corresponding GAPDH value was used to reveal the relative protein expression. (**B**) The upregulation of TPX2 promoted the migration of the A549 cells, whereas its downregulation inhibited the migration of the H1650 cells. (**C**) The upregulation of TPX2 promoted the invasion of the A549 cells, whereas its downregulation inhibited the invasion of the H1650 cells. (**D**) Morphological observations of different treated A549 cells in pseudopod and cell rounding (mean±SD; n=3 in triplicate; ** P<0.01).
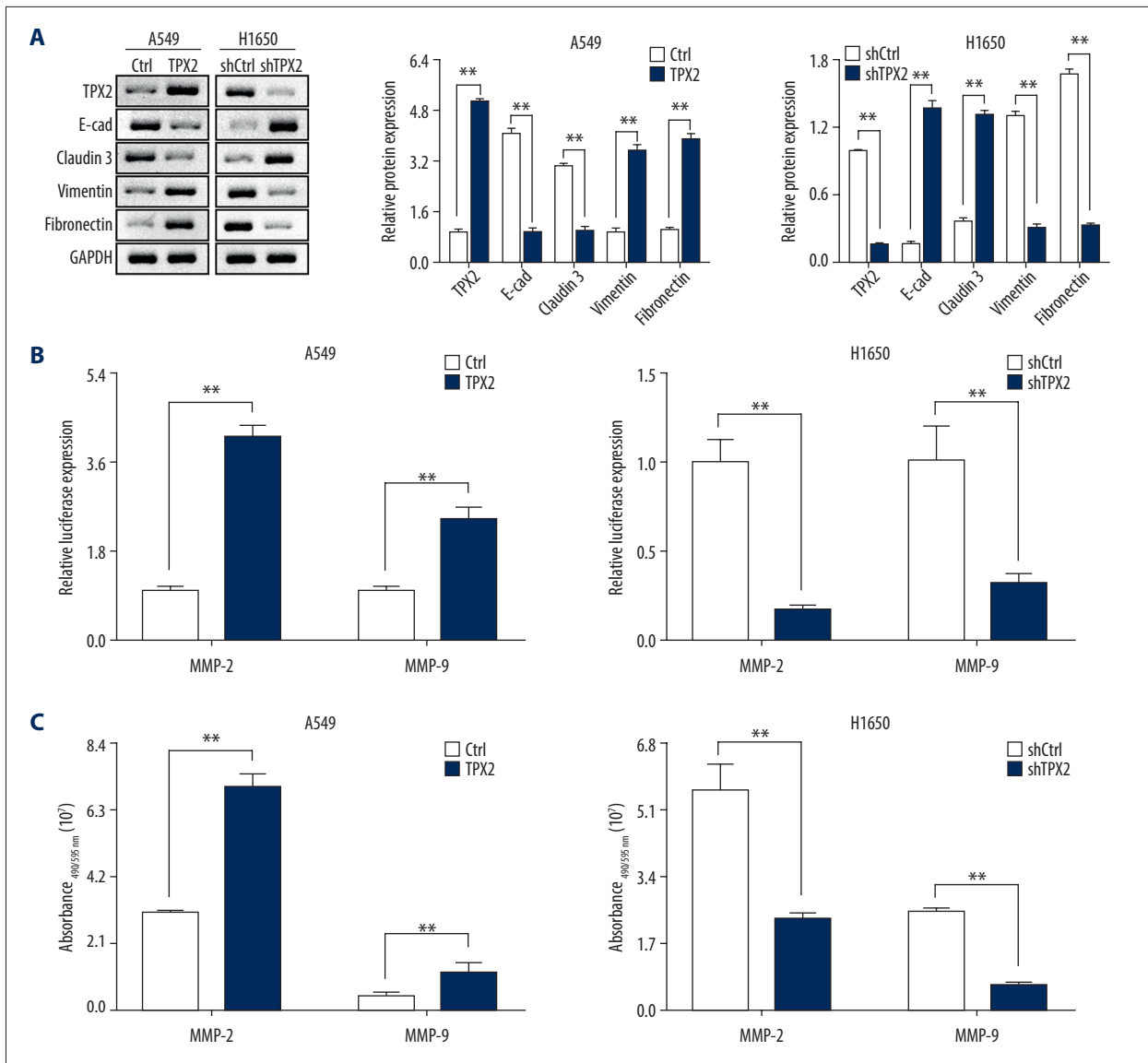
Figure 5. Correlations of TPX2 with EMT and MMPs in NSCLC cells. (**A**) The expression of epithelial marker proteins was consistent with TPX2 content, whereas the expression of mesenchymal marker proteins was opposite the expression of TPX2. (**B**) Luciferase reporter assay results suggested that TPX2 promoted the transcriptional activities of MMP2 and MMP9. (**C**) The enzyme activities of MMP2 and MMP9 were detected by using the activity detecting kit. Expression of both MMP2 and MMP9 activities was significantly higher in the TPX2 overexpression group of A549 cells, whereas in the knockdown group of H1650 cells, the MMP2 and MMP9 activities were significantly decreased when TPX2 was knocked down (mean±SD; n=3 in triplicate; ** P<0.01).

screened as TPX2 low-expression and high-expression models for subsequent experiments (Figure 4A). The wound healing assay showed that after 48 h of treatment, scratch wounds were significantly thinner in the high TPX2 expression groups (Figure 4B). In the Matrigel invasion assay, the passed cells were significantly increased when TPX2 was upregulated in the A549 cells and significantly decreased when TPX2 was knocked down in the H1650 cells (Figure 4C). The morphological results showed notable differences between the control and TPX2 overexpression groups, including pseudopod disappearance and cell rounding (Figure 4D).

TPX2 promotes the EMT process and the expression and activity of MMP2 and MMP9

During the omics analysis, we found significant differences in the regulation of the EMT process and extracellular matrix organization, and we suspected that TPX2 promoted the

metastasis and malignant progression of NSCLC through EMT and MMPs. The Western blot results showed that when TPX2 was upregulated in the A549 cells, the expression of the epithelial marker proteins E-cad and claudin 3 was significantly decreased, whereas the expression of the mesenchymal marker proteins vimentin and fibronectin was significantly increased. Similarly, when TPX2 was knocked down in the H1650 cells, the expression of the epithelial marker proteins was significantly upregulated and that of the mesenchymal marker proteins was significantly downregulated (Figure 5A). In addition, MMP2 and MMP9 transcription was significantly increased after overexpression of TPX2 in A549 cells and significantly decreased when TPX2 was knocked down in H1650 cells (Figure 5B). The results of the MMP activity assays further revealed that the enzyme activities of MMP2 and MMP9 significantly increased with the upregulation of TPX2 in A549 cells and significantly decreased with the downregulation of TPX2 in H1650 cells (Figure 5C).

Discussion

Bioinformatics analysis allows the identification of tumor-associated node genes from large data repositories to assist in the clarification of mechanisms and the prognostic assessment of cancer [15,22]. In the present study, we chose 9 samples of circulating NSCLC tumor cells and 9 samples of nonmetastatic NSCLC tumor cells in a GEO database to identify DEGs. Through further topological network analysis, we screened the node gene *TPX2*. TPX2 is a microtubule-associated protein whose expression is strictly controlled within the cell cycle; it appears during the G1/S stage and vanishes after the completion of cytokinesis [23,24]. Several studies have revealed that overexpression of TPX2 is correlated with tumor proliferation, stage, grade, and survival rate in some malignant tumors [25]. Thus, we speculated that TPX2 might play an important role in the metastasis and malignant progression of NSCLC. Further study verified our hypothesis through the TCGA database, and the results showed that the high expression of TPX2 was significantly positively correlated with metastasis, clinical stage, and poor survival prognosis of NSCLC.

As a microtubule-associated protein, TPX2 has been reported to mediate spindle filament assembly during mitosis and to be related to cell proliferation [23]. Although a number of studies
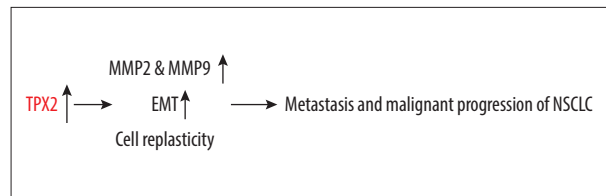
Figure 6. Proposed regulatory mechanism of TPX2 in the metastasis and malignant progression of NSCLC.

have clarified the relationship between TPX2 and tumor apoptosis and metastasis in liver and gastric cancer [16,19], the detailed mechanism of TPX2 in NSCLC remains unclear. In this study, results from omics data analysis showed that the cell adhesion function and EMT process were significantly dysregulated after NSCLC metastasized. Further *in vitro* experiments demonstrated that TPX2 indeed promoted the EMT process and the degradation of extracellular matrix. Meanwhile, morphological observations of TPX2-overexpressed NSCLC cells showed that TPX2 changed the cell shape from a clawed epithelial morphology to one with pseudopod disappearance and cell rounding, with the near-suspended cells remaining viable. We speculated that the regulation of microtubules by TPX2 likely mediated the cytoskeleton remodeling of NSCLC cells, which in turn activated the mesenchymal transition of tumor cells and expression of MMPs and enabled NSCLC cells to metastasize. However, it remained unclear how cytoskeleton remodeling affected the EMT process and MMP-mediated degradation of extracellular matrix, and further research is required.

Conclusions

In summary, this study demonstrated that TPX2 promoted NSCLC metastasis and malignant progression. The effects of TPX2 in NSCLC may have been mediated through regulation of cytoskeleton remodeling as well as the further activation of the EMT process and MMP expression and enzyme activities (Figure 6). TPX2 might serve as a marker of metastasis and poor prognosis in NSCLC, and it could potentially serve as a target for the clinical treatment of NSCLC.

Conflict of interest

None.

Supplementary Data

Supplementary Table 1. The TCGA and Protein Atlas – downloaded data.

Sample	FPKM TPX2	AJCC pathologic m	AJCC pathologic n
TCGA-78-7167	0.8	M1	N0
TCGA-49-4510	1.1	M0	N1
TCGA-55-8512	1.2	M1b	N1
TCGA-86-A4P8	1.2	MX	N2
TCGA-78-7156	1.5	M1	N1
TCGA-91-6849	1.7	MX	N2
TCGA-67-6217	1.9	M0	N1
TCGA-91-A4BD	2.1	MX	N1
TCGA-NJ-A7XG	2.2	M0	N1
TCGA-05-4384	2.6	M0	N2
TCGA-MP-A4T6	3.2	MX	N2
TCGA-05-5423	3.3	M0	N1
TCGA-64-1680	3.4	M1	N2
TCGA-44-2659	3.6	M0	N1
TCGA-L9-A50W	3.6	MX	N1
TCGA-49-4505	3.7	M0	N1
TCGA-69-8253	4	MX	N1
TCGA-NJ-A4YI	4	M0	N2
TCGA-50-5068	4.3	MX	N1
TCGA-86-7714	4.4	M0	N2
TCGA-J2-8192	4.5	MX	N1
TCGA-75-6212	4.6	M0	N1
TCGA-49-4490	4.8	M0	N2
TCGA-44-2665	5.1	M0	N1
TCGA-NJ-A55O	5.3	M0	N1
TCGA-38-4627	5.4	M0	N1
TCGA-55-6983	5.7	M0	N1
TCGA-55-7227	5.7	MX	N1
TCGA-73-4675	5.7	M0	N1
TCGA-97-8171	5.8	M1a	N2
TCGA-50-5055	5.9	M0	N1
TCGA-86-8671	6.3	M0	N1
TCGA-86-8674	6.3	M0	N1
TCGA-86-8359	6.4	M0	N2
TCGA-50-5932	6.5	M0	N1
TCGA-86-8278	6.6	M0	N1
TCGA-49-6744	6.9	MX	N1
TCGA-78-7158	7.3	M0	N1
TCGA-05-5428	7.4	M0	N1

Sample	FPKM TPX2	AJCC pathologic m	AJCC pathologic n
TCGA-50-5045	7.5	M0	N1
TCGA-49-4506	7.8	M0	N1
TCGA-62-A46Y	7.8	M0	N2
TCGA-97-8547	8.2	MX	N2
TCGA-38-4628	8.3	M0	N1
TCGA-05-4396	8.6	M0	N1
TCGA-55-7283	8.6	MX	N2
TCGA-MP-A4TD	8.6	M0	N2
TCGA-53-7626	9.3	M0	N1
TCGA-55-6984	9.3	M0	N1
TCGA-95-A4VK	9.3	M0	N2
TCGA-49-4512	9.4	MX	N2
TCGA-55-7914	9.4	MX	N1
TCGA-55-A48X	9.5	M0	N1
TCGA-05-5420	9.6	M0	N2
TCGA-55-8094	10.2	M1b	N0
TCGA-MP-A4T9	10.2	MX	N2
TCGA-78-7160	10.3	M1	N2
TCGA-91-6830	10.7	MX	N1
TCGA-05-4402	10.9	M1	NX
TCGA-05-4425	11.1	M1	N0
TCGA-86-8279	11.1	M0	N1
TCGA-93-A4JP	11.3	M1b	NX
TCGA-55-8615	11.3	MX	N2
TCGA-44-6774	11.6	M0	N2
TCGA-49-AAQV	11.6	MX	N1
TCGA-97-7554	11.6	M0	N2
TCGA-05-4418	12	M0	N2
TCGA-50-5051	12	M0	N2
TCGA-55-8508	12	MX	N1
TCGA-05-5429	12.3	M0	N2
TCGA-50-5930	12.8	M0	N2
TCGA-64-5815	13	M0	N1
TCGA-L9-A5IP	13.1	M1b	N2
TCGA-78-7148	13.1	M0	N1
TCGA-55-7907	13.3	MX	N1
TCGA-86-6851	13.4	M0	N1
TCGA-MP-A4SY	13.5	M0	N1
TCGA-MP-A4T8	13.5	M0	N2

Sample	FPKM TPX2	AJCC pathologic m	AJCC pathologic n
TCGA-55-8505	13.7	MX	N2
TCGA-MP-A4SW	13.8	M0	N1
TCGA-73-4659	13.9	M0	N2
TCGA-50-6593	14	M0	N2
TCGA-86-8055	14.2	M0	N1
TCGA-78-7166	14.4	M0	N1
TCGA-L9-A7SV	14.4	M0	N1
TCGA-55-6981	14.5	M0	N2
TCGA-95-A4VP	14.7	M0	N2
TCGA-L9-A743	14.7	M0	N2
TCGA-44-3396	14.8	M0	N2
TCGA-78-7147	15	M0	N1
TCGA-95-7567	15	M0	N1
TCGA-55-6970	15.3	MX	N2
TCGA-55-6982	15.4	M0	N1
TCGA-99-8025	15.5	M0	N2
TCGA-MP-A4T7	16	M1	N0
TCGA-49-AAR4	16.2	MX	N2
TCGA-55-A48Z	17.4	MX	N3
TCGA-55-6712	17.8	MX	N1
TCGA-64-1679	18	M0	N2
TCGA-49-6745	18.3	M0	N2
TCGA-62-8398	18.3	M0	N2
TCGA-49-4494	18.6	M0	N2
TCGA-78-8640	18.8	M0	N1
TCGA-86-8074	18.8	M0	N1
TCGA-78-7145	19.3	M1	N1
TCGA-99-8033	19.4	M1	NX
TCGA-86-6562	19.5	M0	N1
TCGA-73-4668	19.7	M0	N1
TCGA-05-4434	20	M1	N1
TCGA-49-6761	20.7	MX	N2
TCGA-69-7974	21.1	MX	N2
TCGA-MP-A4TK	21.2	MX	N1
TCGA-38-4632	21.4	M1	N1
TCGA-64-5779	21.6	M0	N2
TCGA-50-5941	21.8	M0	N2
TCGA-73-4676	21.8	M0	N1
TCGA-62-8399	21.9	M0	N2
TCGA-MN-A4N1	22	M0	N1
TCGA-35-5375	22.5	M0	N2
TCGA-95-7562	22.5	M0	N1

Sample	FPKM TPX2	AJCC pathologic m	AJCC pathologic n
TCGA-69-7978	22.6	MX	N1
TCGA-55-6979	23.1	M0	N1
TCGA-MP-A4T4	23.3	M0	N1
TCGA-64-1677	23.5	M0	N2
TCGA-53-A4EZ	23.7	MX	N1
TCGA-05-4432	24.1	M0	N1
TCGA-49-4507	24.4	M0	N1
TCGA-55-1596	24.4	M0	N1
TCGA-95-A4VN	24.4	M0	N1
TCGA-50-5044	24.6	M0	N1
TCGA-97-8176	24.7	M0	N1
TCGA-05-4398	25.3	M0	N3
TCGA-73-4670	25.4	M1	N0
TCGA-62-8402	25.9	M0	N2
TCGA-55-7727	26.2	MX	N2
TCGA-50-5936	26.3	M0	N2
TCGA-50-5933	26.6	M0	N2
TCGA-62-A471	26.7	M0	N1
TCGA-50-6594	27.1	M0	N2
TCGA-86-8054	27.8	M0	N1
TCGA-86-7711	28.4	M0	N1
TCGA-78-7150	29.3	M0	N1
TCGA-05-5425	29.6	M0	N1
TCGA-93-A4JN	29.7	M1a	N0
TCGA-MP-A4TC	29.8	M0	N2
TCGA-MP-A4TI	30.2	M0	N1
TCGA-95-8494	30.8	M0	N1
TCGA-49-6742	31	M0	N1
TCGA-86-7701	31.2	M1	N0
TCGA-55-1594	32.7	M0	N2
TCGA-78-7220	34.3	M0	N2
TCGA-62-8394	34.4	M0	N2
TCGA-55-6975	34.5	M0	N1
TCGA-05-4250	36.7	M0	N1
TCGA-78-7154	36.7	M0	N2
TCGA-05-4415	36.9	M0	N2
TCGA-50-5072	37.2	M0	N2
TCGA-44-5643	38.9	M0	N2
TCGA-05-4427	40	M0	N1
TCGA-55-5899	40.1	M0	N1
TCGA-50-6591	41	M1	N0
TCGA-49-6743	41.8	MX	N2

Sample	FPKM TPX2	AJCC pathologic m	AJCC pathologic n
TCGA-49-AAR3	42	MX	N1
TCGA-78-8660	42.1	M0	N1
TCGA-44-7669	42.3	MX	N1
TCGA-75-5125	45.1	M0	N1
TCGA-50-6595	46.6	M0	N2
TCGA-75-6214	46.9	M0	N2
TCGA-44-6779	49.2	MX	N1
TCGA-73-4666	53.1	M1	N0
TCGA-55-8620	58.5	M1b	N1
TCGA-78-7536	62.8	M0	N2
TCGA-44-7670	63.6	M0	N1
TCGA-05-4397	64.5	M0	N1
TCGA-91-6848	64.6	MX	N2
TCGA-55-6968	65.9	M1	N0
TCGA-78-7146	74.3	M0	N2
TCGA-53-7624	75.6	M1	N0
TCGA-44-6148	0.8	M0	N0
TCGA-67-3773	1.1	M0	N0
TCGA-78-7163	1.3	M0	N0
TCGA-49-4486	1.4	M0	N0
TCGA-50-5942	1.4	M0	N0
TCGA-35-3615	1.5	M0	N0
TCGA-50-8457	1.5	M0	N0
TCGA-75-6206	1.5	M0	N0
TCGA-78-7537	1.6	M0	N0
TCGA-97-A4M1	1.6	M0	N0
TCGA-L4-A4E6	1.7	M0	N0
TCGA-73-7498	1.8	M0	N0
TCGA-75-5146	1.9	M0	N0
TCGA-75-7025	1.9	M0	N0
TCGA-62-8397	2	M0	N0
TCGA-97-A4M2	2	M0	N0
TCGA-MP-A4TH	2	M0	N0
TCGA-97-8174	2.2	M0	N0
TCGA-67-4679	2.3	M0	N0
TCGA-55-8206	2.4	M0	N0
TCGA-73-4677	2.4	M0	N0
TCGA-44-2655	2.5	M0	N0
TCGA-67-3770	2.5	M0	N0
TCGA-38-A44F	2.6	M0	N0
TCGA-55-6980	2.6	M0	N0
TCGA-62-8395	2.6	M0	N0

Sample	FPKM TPX2	AJCC pathologic m	AJCC pathologic n
TCGA-62-A46S	2.6	M0	N0
TCGA-99-AA5R	2.6	M0	N0
TCGA-S2-AA1A	2.6	M0	N0
TCGA-44-3398	2.8	M0	N0
TCGA-67-3774	2.8	M0	N0
TCGA-44-2661	2.9	M0	N0
TCGA-86-8056	2.9	M0	N0
TCGA-50-8460	3.1	M0	N0
TCGA-69-7763	3.1	M0	N0
TCGA-78-7161	3.1	M0	N0
TCGA-86-8076	3.1	M0	N0
TCGA-97-A4M3	3.1	M0	N0
TCGA-78-7539	3.2	M0	N0
TCGA-97-A4M0	3.2	M0	N0
TCGA-NJ-A55A	3.2	M0	N0
TCGA-44-6146	3.3	M0	N0
TCGA-78-7633	3.3	M0	N0
TCGA-78-7149	3.5	M0	N0
TCGA-78-7540	3.5	M0	N0
TCGA-MP-A5C7	3.5	M0	N0
TCGA-50-5935	3.7	M0	N0
TCGA-67-3772	3.7	M0	N0
TCGA-86-8668	3.7	M0	N0
TCGA-86-A456	3.7	M0	N0
TCGA-05-4403	3.9	M0	N0
TCGA-49-4501	3.9	M0	N0
TCGA-78-7162	3.9	M0	N0
TCGA-99-7458	3.9	M0	N0
TCGA-05-4249	4	M0	N0
TCGA-38-4626	4.1	M0	N0
TCGA-95-7948	4.1	M0	N0
TCGA-NJ-A4YG	4.1	M0	N0
TCGA-50-6597	4.2	M0	N0
TCGA-50-5944	4.3	M0	N0
TCGA-50-8459	4.4	M0	N0
TCGA-62-A46P	4.5	M0	N0
TCGA-55-6972	4.6	M0	N0
TCGA-97-A4M6	4.6	M0	N0
TCGA-97-8177	4.7	M0	N0
TCGA-97-A4M5	4.7	M0	N0
TCGA-05-4405	5	M0	N0
TCGA-05-4422	5.1	M0	N0

Sample	FPKM TPX2	AJCC pathologic m	AJCC pathologic n
TCGA-44-7671	5.1	M0	N0
TCGA-55-6986	5.1	M0	N0
TCGA-97-8172	5.2	M0	N0
TCGA-44-2666	5.3	M0	N0
TCGA-38-7271	5.4	M0	N0
TCGA-55-A57B	5.4	M0	N0
TCGA-78-8655	5.4	M0	N0
TCGA-73-4662	5.6	M0	N0
TCGA-86-8669	5.6	M0	N0
TCGA-44-8120	6	M0	N0
TCGA-86-8280	6.1	M0	N0
TCGA-97-A4M7	6.2	M0	N0
TCGA-44-2656	6.3	M0	N0
TCGA-44-8117	6.3	M0	N0
TCGA-64-1681	6.3	M0	N0
TCGA-99-8028	6.4	M0	N0
TCGA-67-6216	6.7	M0	N0
TCGA-86-A4P7	6.7	M0	N0
TCGA-05-4426	6.8	M0	N0
TCGA-64-1676	6.8	M0	N0
TCGA-55-7281	7.1	M0	N0
TCGA-55-7574	7.5	M0	N0
TCGA-55-8090	7.6	M0	N0
TCGA-73-4658	7.7	M0	N0
TCGA-71-6725	7.8	M0	N0
TCGA-78-7153	7.9	M0	N0
TCGA-55-8616	8	M0	N0
TCGA-44-3918	8.1	M0	N0
TCGA-67-6215	8.2	M0	N0
TCGA-62-A470	8.7	M0	N0
TCGA-MN-A4N4	8.7	M0	N0
TCGA-05-5715	9.1	M0	N0
TCGA-44-4112	9.2	M0	N0
TCGA-44-A47G	9.4	M0	N0
TCGA-69-7764	9.4	M0	N0
TCGA-62-A46V	9.5	M0	N0
TCGA-78-7152	9.6	M0	N0
TCGA-05-4430	10.4	M0	N0
TCGA-97-A4LX	10.4	M0	N0
TCGA-MN-A4N5	10.5	M0	N0
TCGA-86-8073	10.8	M0	N0
TCGA-44-A47B	11.1	M0	N0
TCGA-99-8032	11.1	M0	N0
TCGA-05-4417	11.2	M0	N0
TCGA-NJ-A4YP	11.2	M0	N0
TCGA-55-6987	11.4	M0	N0
TCGA-62-A46R	11.4	M0	N0
TCGA-69-7760	11.5	M0	N0
TCGA-64-5778	11.6	M0	N0
TCGA-69-7980	11.6	M0	N0
TCGA-86-7954	11.7	M0	N0
TCGA-71-8520	11.9	M0	N0
TCGA-05-4433	12	M0	N0
TCGA-55-A48Y	12	M0	N0
TCGA-MP-A4TJ	12	M0	N0
TCGA-78-8648	12.2	M0	N0
TCGA-55-8203	12.5	M0	N0
TCGA-97-8179	12.5	M0	N0
TCGA-97-8175	12.8	M0	N0
TCGA-NJ-A4YF	12.9	M0	N0
TCGA-NJ-A4YQ	13	M0	N0
TCGA-62-A472	13.1	M0	N0
TCGA-80-5608	13.2	M0	N0
TCGA-L4-A4E5	13.2	M0	N0
TCGA-50-5049	13.4	M0	N0
TCGA-50-5066	14.1	M0	N0
TCGA-50-6673	14.2	M0	N0
TCGA-75-5147	15.2	M0	N0
TCGA-91-6828	15.2	M0	N0
TCGA-50-7109	15.3	M0	N0
TCGA-MP-A4TF	15.4	M0	N0
TCGA-44-6145	15.7	M0	N0
TCGA-4B-A93V	15.8	M0	N0
TCGA-35-4123	15.9	M0	N0
TCGA-86-8075	15.9	M0	N0
TCGA-05-4389	16.5	M0	N0
TCGA-55-1592	16.6	M0	N0
TCGA-05-4382	16.7	M0	N0
TCGA-35-4122	16.7	M0	N0
TCGA-64-5781	16.7	M0	N0
TCGA-91-6835	16.7	M0	N0
TCGA-44-A4SS	16.8	M0	N0
TCGA-86-8672	16.9	M0	N0
TCGA-50-5939	17.8	M0	N0

Sample	FPKM TPX2	AJCC pathologic m	AJCC pathologic n
TCGA-55-8085	17.9	M0	N0
TCGA-44-3919	18	M0	N0
TCGA-69-A59K	18.2	M0	N0
TCGA-86-7713	18.5	M0	N0
TCGA-78-8662	18.7	M0	N0
TCGA-44-7672	19.6	M0	N0
TCGA-95-7944	19.8	M0	N0
TCGA-64-1678	20.2	M0	N0
TCGA-78-7535	20.2	M0	N0
TCGA-53-7813	20.3	M0	N0
TCGA-55-8208	20.7	M0	N0
TCGA-86-7953	20.8	M0	N0
TCGA-67-3771	21.4	M0	N0
TCGA-55-7910	21.6	M0	N0
TCGA-86-A4JF	21.9	M0	N0
TCGA-73-7499	22.9	M0	N0
TCGA-38-4629	23.1	M0	N0
TCGA-05-4390	23.5	M0	N0
TCGA-44-3917	24.1	M0	N0
TCGA-05-4420	24.2	M0	N0
TCGA-86-8585	25	M0	N0
TCGA-55-7576	25.8	M0	N0
TCGA-44-8119	27	M0	N0
TCGA-91-6840	28	M0	N0
TCGA-69-7973	28.3	M0	N0

Sample	FPKM TPX2	AJCC pathologic m	AJCC pathologic n
TCGA-95-7947	28.3	M0	N0
TCGA-78-7143	28.5	M0	N0
TCGA-69-8255	29	M0	N0
TCGA-75-7027	29	M0	N0
TCGA-44-2662	30	M0	N0
TCGA-MP-A4SV	30.2	M0	N0
TCGA-49-4514	31	M0	N0
TCGA-55-8089	31.4	M0	N0
TCGA-86-8673	31.9	M0	N0
TCGA-44-7661	34	M0	N0
TCGA-62-A46O	35.8	M0	N0
TCGA-86-7955	36.1	M0	N0
TCGA-64-5775	36.3	M0	N0
TCGA-86-A4D0	36.4	M0	N0
TCGA-50-5931	37	M0	N0
TCGA-38-4631	37.5	M0	N0
TCGA-MP-A4TA	37.7	M0	N0
TCGA-50-6592	39.9	M0	N0
TCGA-80-5611	40.8	M0	N0
TCGA-64-5774	43.9	M0	N0
TCGA-05-4424	47.4	M0	N0
TCGA-73-A9RS	49.3	M0	N0
TCGA-55-8205	52.2	M0	N0
TCGA-78-7542	52.4	M0	N0

References:

1. Bray F, Ferlay J, Soerjomataram I et al: Global cancer statistics 2018: GLOBOCAN estimates of incidence and mortality worldwide for 36 cancers in 185 countries. Cancer J Clin, 2018; 68(6): 394–424

2. Vesel M, Rapp J, Feller D et al: ABCB1 and ABCG2 drug transporters are differentially expressed in non-small cell lung cancers (NSCLC) and expression is modified by cisplatin treatment via altered Wnt signaling. Respir Res, 2017; 18(1): 52

3. Jamal-Hanjani M, Wilson GA, McGranahan N et al: Tracking the evolution of non-small-cell lung cancer. N Engl J Med, 2017; 376: 2109–21

4. Miller KD, Nogueira L, Mariotto AB et al: Cancer treatment and survivorship statistics, 2019. Cancer J Clin, 2019; 69: 363–85

5. Zaroulidis K, Zarogoulidis P, Darwiche K et al: Treatment of non-small cell lung cancer (NSCLC). J Thorac Dis, 2013; 5(Suppl. 4): S389–96

6. Yoon SM, Shaikh T, Hallman M: Therapeutic management options for stage III non-small cell lung cancer. World J Clin Oncol, 2017; 8: 1–20

7. Elsayad K, Samhouri L, Scobioala S et al: Is tumor volume reduction during radiotherapy prognostic relevant in patients with stage III non-small cell lung cancer? J Cancer Res Clin Oncol, 2018; 144: 1165–71

8. Shi L, He Y, Yuan Z et al: Radiomics for response and outcome assessment for non-small cell lung cancer. Technol Cancer Res Treat, 2018; 17: 1533033818782788

9. Antonia SJ, Villegas A, Daniel D et al: Durvalumab after chemoradiotherapy in stage III non-small-cell lung cancer. N Engl J Med, 2017; 377: 1919–29

10. Plaks V, Koopman CD, Werb Z: Cancer. Circulating tumor cells. Science, 2013; 341: 1186–88

11. Li H, Zhao X, Wang J et al: Bioinformatics analysis of gene expression profile data to screen key genes involved in pulmonary sarcoidosis. Gene, 2017; 596: 98–104

12. Huang Y, Tao Y, Li X et al: Bioinformatics analysis of key genes and latent pathway interactions based on the anaplastic thyroid carcinoma gene expression profile. Oncol Lett, 2017; 13: 167–76

13. Jiang W, Liu P, Zhang J, Yang W: Identification of key candidate genes and pathways of Candida albicans-infected human umbilical vein endothelial cells and drug screening. Indian J Microbiol, 2020; 60: 62–69

14. Mishra DK, Creighton CJ, Zhang Y et al: Ex vivo four-dimensional lung cancer model mimics metastasis. Ann Thorac Surg, 2015; 99: 1149–56

15. Zhang Q, Qin Y, Zhao J et al: Thymidine phosphorylase promotes malignant progression in hepatocellular carcinoma through pentose Warburg effect. Cell Death Dis, 2019; 10: 43

16. Liang B, Jia C, Huang Y et al: TPX2 level correlates with hepatocellular carcinoma cell proliferation, apoptosis, and EMT. Dig Dis Sci, 2015; 60: 2360–72

17. Yan L, Li Q, Yang J, Qiao B: TPX2-p53-GLIPR1 regulatory circuitry in cell proliferation, invasion, and tumor growth of bladder cancer. J Cell Biochem, 2018; 119: 1791–803

18. Song T, Xu A, Zhang Z et al: CircRNA hsa_circRNA_101996 increases cervical cancer proliferation and invasion through activating TPX2 expression by restraining miR-8075. J Cell Physiol, 2019; 234: 14296–305

19. Liang B, Zheng W, Fang L et al: Overexpressed targeting protein for Xklp2 (TPX2) serves as a promising prognostic marker and therapeutic target for gastric cancer. Cancer Biol Ther, 2016; 17: 824–32

20. Schneider MA, Christopoulos P, Muley T et al: AURKA, DLGAP5, TPX2, KIF11 and CKAP5: Five specific mitosis-associated genes correlate with poor prognosis for non-small cell lung cancer patients. Int J Oncol, 2017; 50: 365–72

21. Yu G, Wang LG et al: clusterProfiler: An R package for comparing biological themes among gene clusters. OMICS, 2012; 16: 284–87

22. Keerthikumar S: An introduction to proteome bioinformatics. Methods Mol Biol, 2017; 1549: 1–3

23. Stewart S, Fang G: Anaphase-promoting complex/cyclosome controls the stability of TPX2 during mitotic exit. Mol Cell Biol, 2005; 25: 10516–27

24. Higuchi T, Uhlmann F: Stabilization of microtubule dynamics at anaphase onset promotes chromosome segregation. Nature, 2005; 433: 171–76

25. Huang C, Han Z, Wu D: Effects of TPX2 gene on radiotherapy sensitization in breast cancer stem cells. Oncol Lett, 2017; 14: 1531–35